

See discussions, stats, and author profiles for this publication at: <https://www.researchgate.net/publication/45422687>

Transition from Tunneling to Hopping in Single Molecular Junctions by Measuring Length and Temperature Dependence

ARTICLE *in* JOURNAL OF THE AMERICAN CHEMICAL SOCIETY · AUGUST 2010

Impact Factor: 12.11 · DOI: 10.1021/ja1040946 · Source: PubMed

CITATIONS

72

READS

115

9 AUTHORS, INCLUDING:



Thomas Hines

Arizona State University

7 PUBLICATIONS 167 CITATIONS

SEE PROFILE



Ismael Diez-Perez

University of Barcelona

69 PUBLICATIONS 1,537 CITATIONS

SEE PROFILE



Hongmei Liu

Linyi University

40 PUBLICATIONS 567 CITATIONS

SEE PROFILE



Zhong-Sheng Wang

Fudan University

107 PUBLICATIONS 7,124 CITATIONS

SEE PROFILE

Transition from Tunneling to Hopping in Single Molecular Junctions by Measuring Length and Temperature Dependence

Thomas Hines,[†] Ismael Diez-Perez,[†] Joshua Hihath,[†] Hongmei Liu,[‡]
Zhong-Sheng Wang,[§] Jianwei Zhao,^{*,‡} Gang Zhou,^{*,§} Klaus Müllen,^{*,||} and
Nongjian Tao^{*,†}

Center for Biosensors and Bioelectronics, Biodesign Institute, Arizona State University, Tempe, Arizona 85287, Key Laboratory of Analytical Chemistry for Life Science (MOE), School of Chemistry and Chemical Engineering, Nanjing University, Nanjing 210008, China, Laboratory of Advanced Materials, Fudan University, Shanghai 200438, China, and Max-Planck-Institute for Polymer Research, Ackermannweg 10, D-55128 Mainz, Germany

Received May 12, 2010; E-mail: Nongjian.Tao@asu.edu; zhougang@fudan.edu.cn; zhaojw@nju.edu.cn; muellen@mpip-mainz.mpg.de

Abstract: The charge transport characteristics of a family of long conjugated molecular wires have been studied using the scanning tunneling microscope break junction technique. The family consists of four wires ranging from 3.1 to 9.4 nm in length. The two shortest wires show highly length dependent and temperature invariant conductance behavior, whereas the longer two wires show weakly length dependent and temperature variant behavior. This trend is consistent with a model whereby conduction occurs by two different mechanisms in the family of wires: by a coherent tunneling mechanism in the shorter two and by an incoherent charge hopping process in the longer wires. The temperature dependence of the two conduction mechanisms gives rise to a phenomenon whereby at elevated temperatures longer molecules that conduct via charge hopping can yield a higher conductance than shorter wires that conduct via tunneling. The evolution of molecular junctions as the tip retracts has been studied and explained in context of the characteristics of individual transient current decay curves.

Introduction

Understanding charge transport in a single molecule bridged between two electrodes is paramount to the goal of creating devices from single molecules and directly relevant to electron transfer phenomena in many chemical and biological systems.^{1,2} Two distinct charge transport mechanisms have been extensively discussed in the literature: coherent transport via tunneling or superexchange and incoherent thermally activated hopping. Coherent tunneling or superexchange dominates through short molecules, and the conductance is given by³

$$G = G_c e^{-\beta L} \quad (1)$$

where G_c is the contact conductance, β is the tunneling decay constant, and L is the length of the molecule. In addition to the exponential decay of the conductance with molecular length, this coherent process is characterized by temperature independence. Incoherent hopping is believed to be responsible for charge transport along long molecular wires, and the conductance follows an Arrhenius relation given by

$$G \propto \exp\left(\frac{-E_A}{k_B T}\right) \quad (2)$$

where E_A represents the hopping activation energy. Charge hopping is also characterized as a weakly length dependent process which gives rise to conductance that varies as the inverse of molecular length.

Wirelike molecules made of repeating units are ideal for understanding charge transport mechanisms because they allow one to study both coherent and incoherent transport as well as the transition between the two by systematically changing the wire length. The transition from tunneling to hopping was observed by measuring photoinduced charge transfer kinetics in donor–bridge–acceptor systems with modulated molecular length⁴ and in DNA molecules.⁵ Theoretical works by various groups^{6–12} have provided additional insights into the experimental results and charge transport mechanisms in general.

[†] Arizona State University.

[‡] Nanjing University.

[§] Fudan University.

^{||} Max-Planck-Institute for Polymer Research.

(1) Nitzan, A.; Ratner, M. A. *Science* **2003**, *300* (5624), 1384–1389.

(2) Tao, N. J. *Nat. Nanotechnol.* **2006**, *1* (3), 173–181.

(3) Magoga, M.; Joachim, C. *Phys. Rev. B* **1998**, *57* (3), 1820–1823.

(4) Davis, W. B.; Svec, W. A.; Ratner, M. A.; Wasielewski, M. R. *Nature* **1998**, *396* (6706), 60–63.

(5) Giese, B.; Amaudrut, J.; Kohler, A. K.; Spormann, M.; Wessely, S. *Nature* **2001**, *412* (6844), 318–320.

(6) Davis, W. B.; Wasielewski, M. R.; Ratner, M. A.; Mujica, V.; Nitzan, A. *J. Phys. Chem. A* **1997**, *101* (35), 6158–6164.

(7) Segal, D.; Nitzan, A.; Ratner, M.; Davis, W. B. *J. Phys. Chem. B* **2000**, *104* (13), 2790–2793.

(8) Joachim, C.; Ratner, M. A. *Proc. Natl. Acad. Sci. U.S.A.* **2005**, *102* (25), 8801–8808.

(9) Nitzan, A. *Annu. Rev. Phys. Chem.* **2001**, *52*, 681–750.

(10) Petrov, E. G.; Shevchenko, Y. V.; Teslenko, V. I.; May, V. *J. Chem. Phys.* **2001**, *115* (15), 7107–7122.

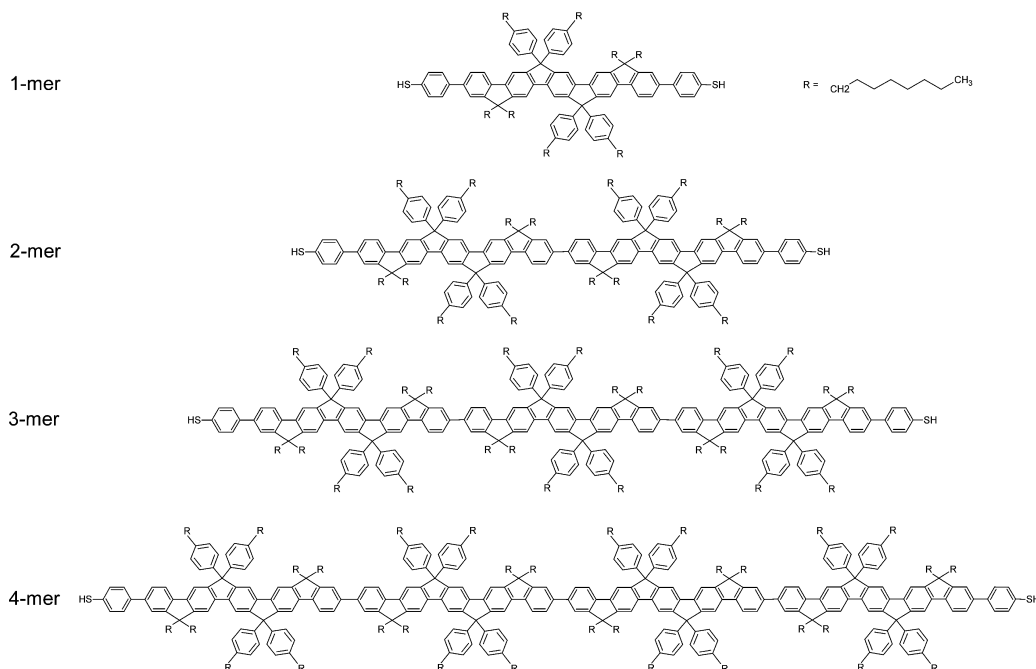


Figure 1. Molecular structure of the wires used in this study. The lengths measure 3.1, 5.2, 7.3, and 9.4 nm for the 1-, 2-, 3-, and 4-mer wires, respectively.

Few conductance measurements of molecules with modulated length bridged between electrodes have been carried out. Xu et al. reported a hopping-like charge transport mechanism based on length dependence measurements in DNA molecules containing GC base pairs.¹³ However, further work did not show a strong temperature dependence in these DNA molecules due to the narrow temperature window accessible for the experiment.¹⁴ Frisbie and colleagues first reported on the transition from tunneling to hopping by means of direct resistive measurements as a function of molecular length, temperature, and applied bias in junctions made out of hundreds of molecules using conducting probe atomic force microscopy (CP-AFM).¹⁵ The experiment was carried out in molecular thin films in which short-range intermolecular interactions prevent these results from being directly correlated with the behavior of a single molecule.¹⁶ Wang and colleagues first reported on the mechanism transition at the single-molecule level by characterizing the distance dependence of molecular conductance using the scanning tunneling microscopy (STM) break junction method and CP-AFM;¹⁷ however, the results were reported only in light of length dependence, not temperature dependence, which is necessary to be completely certain that a transition from tunneling to hopping has occurred.¹⁸

Here, we report results that support a transition between tunneling and hopping in single-molecule junctions by carrying

out both length and temperature dependent measurements of conductance. The family of molecules investigated consisted of four molecular wires ranging from 3.1 to 9.4 nm in length, shown in Figure 1. To the best of our knowledge, the last molecule in this family represents the longest molecular wire measured by formation of a single molecule junction. At elevated temperatures one can observe higher conductance in the longer wires that conduct via hopping than in the shorter wires that conduct via tunneling. The formation and evolution during pulling of these long molecular wire junctions with the STM break junction method was studied by analyzing the individual transient current decay curves.

Experimental Section

Chemicals. The molecular wires used in this study were synthesized at the Max-Planck Institute for Polymer Research. Analytical and spectral information can be found in the Supporting Information.

Sample Preparation. Gold substrates were prepared by thermally evaporating 130 nm of 99.9995% Alfa Aesar gold onto freshly cleaved mica slides in a UHV chamber ($\sim 5 \times 10^{-8}$ Torr) and annealing for 3 h at 360 °C to ensure a flat Au(111) surface. Each substrate was flame annealed with hydrogen for approximately 45 s before being placed in the STM cell with pure mesitylene. STM tips were prepared by cutting 0.25 mm 99.998% gold wire from Alfa Aesar. Before addition of the molecules, the sample substrate was imaged in the STM to ensure that there was a clean surface that was free of contamination and that sharp terrace ledges were clearly visible, which is indicative of a sharp tip. Once the surface was experimentally confirmed to be free of contamination, the cell was taken out of the STM chamber and a solution of an approximately 100 μM concentration of the protected molecules in mesitylene was added dropwise to the cell. The acetyl protecting group was self-cleaved when the molecules were added to the STM cell because steps corresponding to formation of a molecular bridge

- (11) Felts, A. K.; Pollard, W. T.; Friesner, R. A. *J. Phys. Chem.* **1995**, *99* (9), 2929–2940.
- (12) Okada, A.; Chernyak, V.; Mukamel, S. *J. Phys. Chem. A* **1998**, *102* (8), 1241–1251.
- (13) Xu, B. Q.; Zhang, P. M.; Li, X. L.; Tao, N. J. *Nano Lett.* **2004**, *4* (6), 1105–1108.
- (14) Hihath, J.; Chen, F.; Zhang, P. M.; Tao, N. J. *J. Phys.: Condens. Matter* **2007**, *19* (21), 215202.
- (15) Choi, S. H.; Kim, B.; Frisbie, C. D. *Science* **2008**, *320* (5882), 1482–1486.
- (16) Landau, A.; Kronik, L.; Nitzan, A. *J. Comput. Theor. Nanosci.* **2008**, *5* (4), 535–544.
- (17) Lu, Q.; Liu, K.; Zhang, H. M.; Du, Z. B.; Wang, X. H.; Wang, F. S. *ACS Nano* **2009**, *3* (12), 3861–3868.

- (18) Goldsmith, R. H.; DeLeon, O.; Wilson, T. M.; Finkelstein-Shapiro, D.; Ratner, M. A.; Wasielewski, M. R. *J. Phys. Chem. A* **2008**, *112* (19), 4410–4414.

were immediately observable when break junction measurements were carried out.

Electrical Measurements. The STM break junction method was employed to repeatedly form molecular junctions between gold electrodes.¹⁹ The current was modulated using a homemade LabVIEW program with two feedback set points. The set points were defined as 10 nA and 1 pA with a bin size of 0.7 pA for the 1-mer wire and 1 nA and 0.1 pA with a bin size of 0.07 pA for the 2-, 3-, and 4-mer wires. The upper set points used for either amplifier were not high enough to form a metallic contact between electrodes; however, a molecular junction was still able to form. The LabVIEW program was used to engage the tip toward the surface until the upper set point current was reached. When this occurred, the tip was retracted. In the absence of molecules, a pure exponential decay in the current with respect to the tip–sample distance is observed. However, when molecules are present, a molecular bridge occasionally forms, which produces a plateau in the transient decay curve corresponding to the approximate current through the molecule. The retraction of the probe continues until it reaches a distance of 2–5 nm beyond the distance corresponding to the low set point current. The additional ramping beyond the minimum set point current was added to make sure that the molecular junction had been completely broken. When the probe has finished retracting, the tapping cycle is repeated so that thousands of decay curves can be recorded.

The STM setup consisted of a Molecular Imaging STM head controlled by a Digital Instruments IIIa controller integrated with a homemade LabVIEW feedback program. A single-stage 1 nA/V amplifier was used to measure the 1-mer wire, and an additional 10× second stage was employed to produce an overall gain of 0.1 nA/V for the 2-, 3-, and 4-mer wires. The sample temperature was controlled using a Peltier stage for the 1-mer wire and a resistive heating stage for the 2-, 3-, and 4-mer wires. For each temperature setting, the system was allowed to stabilize for approximately 20–30 min before measurements were taken to minimize thermally induced drift.

Approximately 5000–15000 decay curves were collected for each molecule at each temperature setting. Typically, more curves needed to be measured for longer molecules because the step yield was relatively low at these lengths. Of the recorded curves, approximately 200–400 decay curves showing steplike features for each measurement setting were selected manually to construct a conductance histogram. Curves with steplike features were easily identified due to the long length of the steps, typically close to 1 nm or more, and the generally clean drop in the step that results from breaking the molecular junction. A full discussion of the selection criteria is given in section 2 of the Supporting Information. Experiments were repeated at two to three different temperatures for each molecular wire to ensure reproducibility of the results. Peaks in the histograms were used to determine the conductance of the single-molecule junctions. The median and full width at half-maximum (fwhm) of the peaks were found by fitting each conductance peak to a Gaussian distribution.

Step length data were extracted from transient decay curves showing steplike features. The ramping rate of the tip was fixed at 20 nm/s for all experiments to avoid ramping rate changes from affecting the stability of the junction.²⁰ When tapping experiments were performed, noise from the use of high bias frequently caused dips in the current below the predetermined minimum set point current. To prevent the tip from prematurely ramping toward the surface before the junction had been completely broken, the piezoelectric actuator was assigned to ramp an additional 2–5 nm after the minimum set point current had been reached. Further distances were used for the longer molecular wires. The step length was determined by measuring the distance between a predetermined

high and low current in each transient decay curve that showed current plateaus corresponding to formation of a molecular junction. Thus, both conductance and step length histograms were compiled from the same set of decay curves with current plateaus. Typically, the high current was chosen to be approximately 3 times the value of the median step height, while the low current was chosen to be about 10% of the median step height. Each transient decay curve was processed through a 1000 Hz low-pass filter to minimize the presence of noise spikes, which can interfere with step length measurement.

Results and Discussion

Conductance of the Molecules. Figure 2 shows conductance histograms for the four molecules at 40 °C. This temperature was chosen to compare all four wires because the yield of forming molecular junctions at lower temperatures is prohibitively low for the 3- and 4-mer wires. The yield increases with temperature, an interesting observation that we will discuss later. The conductance is $9.8 \times 10^{-6} G_0$ for the 1-mer wire with a length of 3.1 nm, where G_0 is the conductance quantum defined as $2e^2/h$ (e is the electron charge and h the Planck constant). The value drops to $4.6 \times 10^{-8} G_0$, more than 200-fold, for the 4-mer wire with a length of 9.4 nm. To the best of our knowledge, the 4-mer wire represents the longest molecule that has been measured with the STM break junction method. The shapes of the peaks in the histograms vary from experiment to experiment; however, experiments taken at the same conditions show reproducible peak locations. The distribution of values observed in conductance histograms is attributed to the statistical nature of the break junction system, which can give rise to different molecule electrode contact geometries^{21–23} and molecular configurations.²³ To measure molecular conductance, relatively large bias voltages between 200 and 1200 mV had to be employed to produce conductance steps that could be differentiated from the background. Ideally, low biases are used because at higher biases the current voltage behavior becomes nonlinear in nature.^{24,25} We can be certain that conduction occurs within the linear regime of current–voltage behavior because conductance histograms for the 4-mer wire taken at three different biases (Figure S5, Supporting Information) all show similar conductance peaks. We can be certain that measurements taken with the shorter 1-, 2-, and 3-mer wires were also in the linear regime of conductance due to the larger energy gaps of the molecules (Figure S7, Supporting Information) and lower applied biases that were used compared to those for the 4-mer wire (Table S1, Supporting Information).

Length Dependence. A semilog plot of conductance as a function of molecular wire length with error bars given by the fwhm of the conductance histograms is given in Figure 3. Note that all except the 4-mer wire data were obtained at 25 °C. For the 1- and 2-mer wires, the conductance is highly length dependent, and an exponential fit of the curve gives a tunneling decay constant of $2.06 \pm 0.09 \text{ nm}^{-1}$, which is similar to the decay constant measured for other conjugated molecular

(19) Xu, B. Q.; Tao, N. J. *J. Science* **2003**, 301 (5637), 1221–1223.

(20) Tsutsui, M.; Shoji, K.; Morimoto, K.; Taniguchi, M.; Kawai, T. *Appl. Phys. Lett.* **2008**, 92 (22), 223110.

(21) Muller, K. H. *Phys. Rev. B* **2006**, 73 (4), 045403.

(22) Basch, H.; Cohen, R.; Ratner, M. A. *Nano Lett.* **2005**, 5 (9), 1668–1675.

(23) Hu, Y. B.; Zhu, Y.; Gao, H. J.; Guo, H. *Phys. Rev. Lett.* **2005**, 95 (15), 156803.

(24) Beebe, J. M.; Kim, B.; Gadzuk, J. W.; Frisbie, C. D.; Kushmerick, J. G. *Phys. Rev. Lett.* **2006**, 97 (2), 026801.

(25) Beebe, J. M.; Kim, B.; Frisbie, C. D.; Kushmerick, J. G. *ACS Nano* **2008**, 2 (5), 827–832.

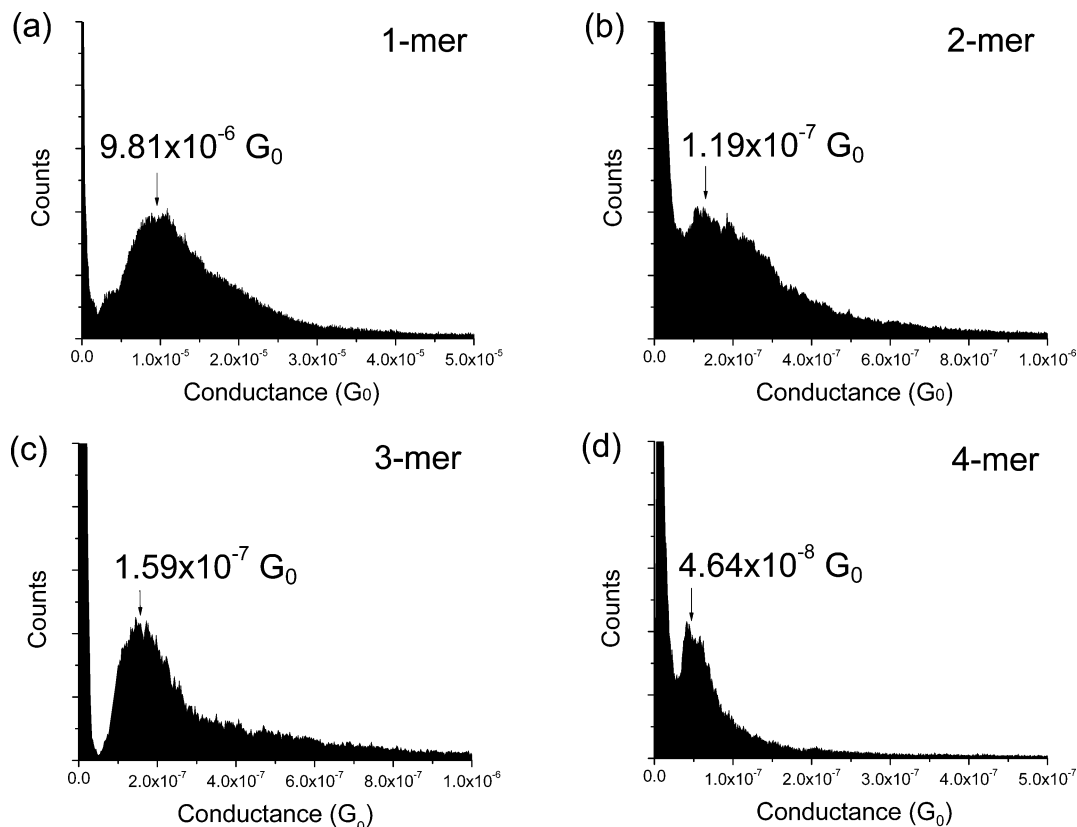


Figure 2. Conductance histograms of each molecular wire at 40 °C. This temperature represents the lowest at which all four wires could be measured.

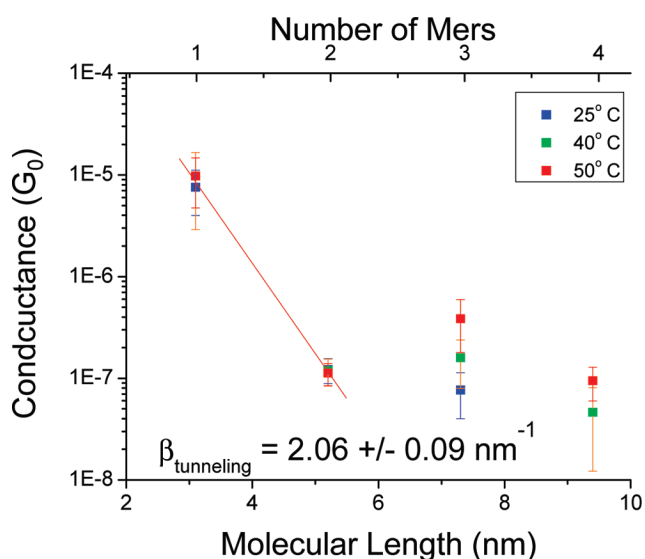


Figure 3. Measured conductance as a function of wire length at $T = 25$, 40, and 50 °C. Conductance was invariant of temperature in the 1- and 2-mer wires and varied systematically with temperature for the 3- and 4-mer wires. The red line is included as a guide to the eye.

wires,^{15,17,26–28} albeit with differing molecular structures. The conductance becomes weakly length dependent for the 3-mer and 4-mer wires. This trend suggests that electron transfer occurs

via a nonresonant tunneling process in the 1- and 2-mer wires and transitions to a charge hopping mechanism for the 3- and 4-mer wires. However, this statement cannot be verified by length dependence alone,¹⁸ and as a result the conductance values of the molecular wires were measured at different temperatures.

Temperature Dependence. Part c of Figure 4 shows that the conductance of the 1- and 2-mer wires is independent of temperature, while parts a and b of Figure 4 show that the conductance of the 3- and 4-mer wires varies systematically with temperature. This trend supports the hypothesis that charge transport occurs by tunneling in the shortest two molecules and by thermally activated hopping in the longer molecules. The transition occurs between the 2- and 3-mer wires for this molecular family, which represents a length of between 5.2 and 7.3 nm. Elsewhere, transitions in other conjugated systems have been approximately 2.5 nm,⁴ 2.75 nm,¹⁷ 4 nm,^{15,28} and from 5.6 to 6.8 nm.²⁶ Thus, compared to other systems, our set of molecular wires display long-range tunneling behavior.

Charge hopping activation energies for the 3- and 4-mer wires were found by fitting Arrhenius curves to Figure 4c. The activation energies for the 3- and 4-mer wires were measured to be 0.52 and 0.58 eV with r^2 values of 0.947 and 0.997, respectively. These values are reasonably consistent with measurements on molecular wires carried out using conducting probe AFM¹⁵ and electrochemical impedance spectroscopy.²⁹

Transition from Tunneling to Hopping. The transition from tunneling to hopping conduction mechanisms leads to a peculiar length dependent conductance for the 2-mer and 3-mer wires. At low temperatures, the shorter 2-mer wire is more conductive

(26) Yamada, R.; Kumazawa, H.; Tanaka, S.; Tada, H. *Appl. Phys. Express* **2009**, 2 (2), 025002.

(27) Salomon, A.; Cahen, D.; Lindsay, S.; Tomfohr, J.; Engelkes, V. B.; Frisbie, C. D. *Adv. Mater.* **2003**, 15 (22), 1881–1890.

(28) Choi, S. H.; Risko, C.; Delgado, M. C. R.; Kim, B.; Bredas, J. L.; Frisbie, C. D. *J. Am. Chem. Soc.* **2010**, 132 (12), 4358–4368.

(29) Arikuma, Y.; Nakayama, H.; Morita, T.; Kimura, S. *Angew. Chem., Int. Ed.* **2010**, 49 (10), 1800–1804.

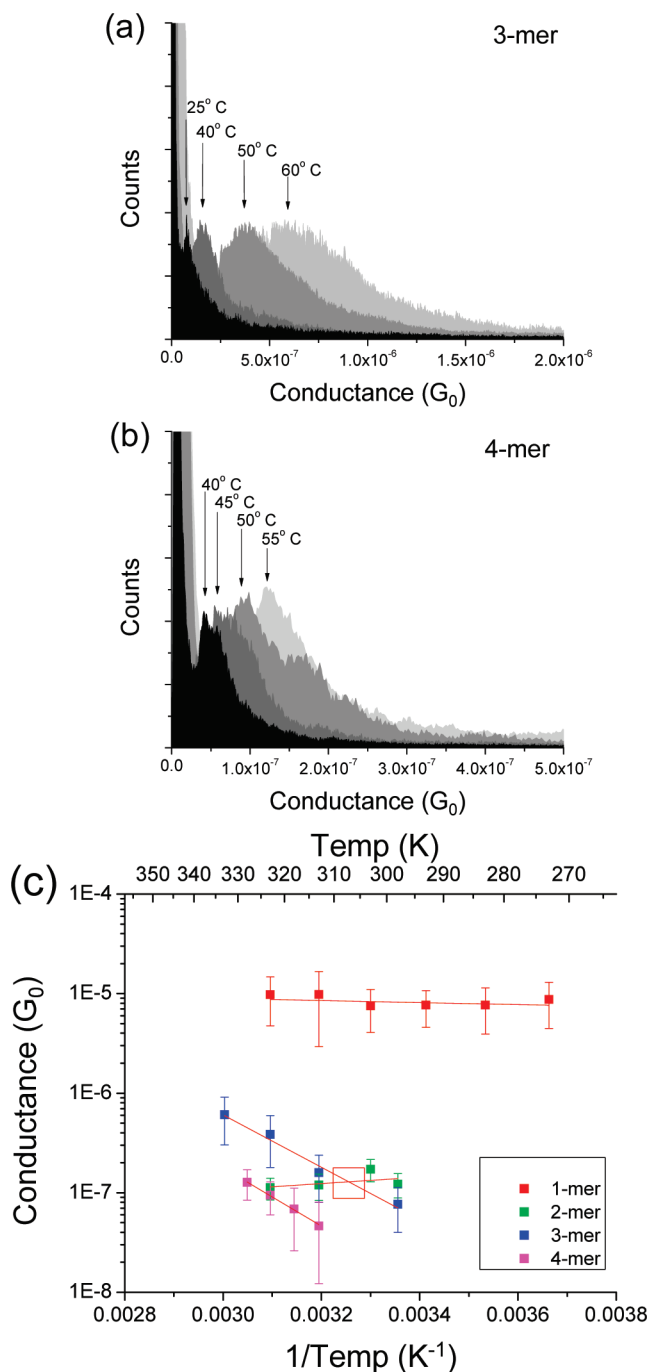


Figure 4. (a, b) Conductance histograms for the 3-mer wire (a) and 4-mer wire (b) measured at different temperatures. (c) Arrhenius plot of conductance for the 1-, 2-, 3-, and 4-mer wires. The conductance values measured for the 3- and 4-mer wires show a systematic dependence on temperature, suggesting that charge transport occurs via a thermally activated hopping process. The red square marks the transition where the conductance of the 3-mer wire intersects the conductance of the 2-mer wire.

than the longer 3-mer wire. However, the 3-mer wire conductance increases with temperature, while the 2-mer wire conductance remains temperature invariant. Consequently, the longer 3-mer wire becomes even more conductive than the shorter 2-mer wire when the temperature is above 40 °C. The crossover point is marked by a red square in Figure 4c. Wasielewski and colleagues observed a similar behavior in the study of photo-excited electron transport in donor–bridge–acceptor molecular

wires.^{4,30} The authors attributed this phenomenon in context of the donor and bridge energy levels and cite the decreasing energy mismatch between the lowest unoccupied molecular orbitals of the donor and bridge as the bridge length increases as being responsible for the higher electron transfer rate in the hopping regime.⁴ Thus, the phenomenon Wasielewski et al. observed was only made possible by the fact that the molecular energy gap changes significantly with the bridge length. However, the absorbance spectrum given in Figure S7 in the Supporting Information shows that the molecular energy gap only decreases from approximately 3.00 to 2.86 eV from the 1-mer to the 4-mer wire. This represents a negligible change compared to that of Wasielewski's wires, and thus, we feel the explanation given by Wasielewski and colleagues does not explain why the hopping conductance can exceed the tunneling conductance in our system.

Molecular Junction Formation. The yield of forming molecular junctions in the present system increases with temperature and decreases with molecular length. The temperature dependence results from the thermal activation required to form a gold–sulfur bond between the STM tip and the terminal thiol group of the molecule. The molecular length dependence of the junction yield results from the relative difficulty in forming a well-ordered SAM with longer molecules. In decay curves where a junction is formed, the steps are frequently defined by fluctuations in the current as the tip retracts (see Figure 5b). This phenomenon has also been observed elsewhere,³¹ and has been attributed to the formation and breakdown of the molecule–electrode contacts. In the present system, the sliding of the molecules on the electrode surfaces during pulling may also contribute to the fluctuations. This phenomenon is discussed in more detail later. Another observation worth noting here is the large step length, the length a molecular junction can be stretched before breakdown. In the case of alkanedithiols, an extensively studied molecular system, the typical step length is a fraction of a nanometer. The step length in the present system can be as large as several nanometers—comparable to the length of the molecules.

Step length information was extracted from transient decay curves collected at 40 °C. Examples of steps collected for the 4-mer wire are given in Figure 5b. This temperature was the lowest at which all four molecular wires could be measured. Length histograms presented in Figure 5c show the step length distributions for all four of the molecular wires. The figure shows a progressive decrease in the median step length as the molecular wire length is increased. This trend is accompanied by a corresponding increase in step length spread as the wire length is increased. Across all wires studied, there were examples of steps approaching the theoretical length of the molecule, measured from sulfur atom to sulfur atom. In fact, in the 3- and 4-mer wires, there were examples of steps exceeding 5 nm in length. The tail end of the step length histogram for the 1-mer wire exceeds the theoretical length of the molecule by as much as 0.75 nm. However, the theoretical length does not include the formation of gold–sulfur bonds at either end of the junction, each of which measure 0.245 nm in length. When these bonds are accounted for, the longest step is only about 0.26 nm longer than the theoretical length of the junction. This length extension can be explained by the formation of a gold atom chain at either

(30) Davis, W. B.; Ratner, M. A.; Wasielewski, M. R. *J. Am. Chem. Soc.* **2001**, *123* (32), 7877–7886.

(31) Huang, Z. F.; Chen, F.; Bennett, P. A.; Tao, N. J. *J. Am. Chem. Soc.* **2007**, *129* (43), 13225–13231.

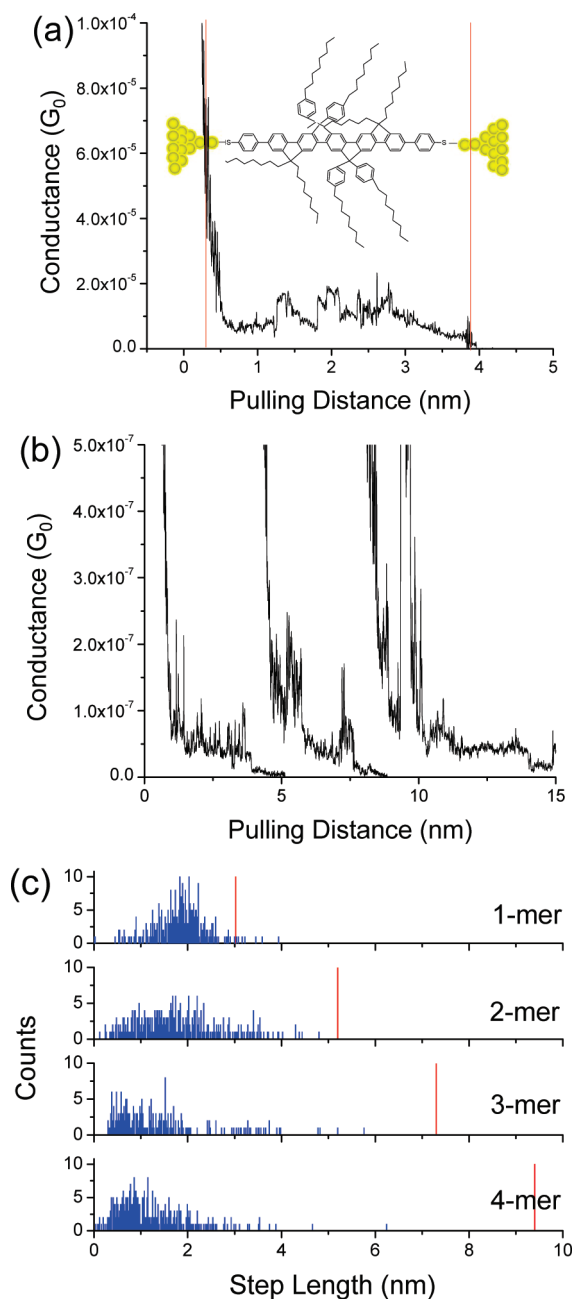


Figure 5. (a) Schematic illustration of 1-mer pulling, which can form steps slightly longer than the molecular length when formation of gold chains at the electrodes is accounted for. The measured length of the step is illustrated by vertical red lines. (b) Transient decay curves of the 4-mer wire, where the step length can exceed 5 nm in length. (c) Histograms of measured step lengths for all four wires at 40 °C. The red lines denote the lengths of the molecular wires.

end of the junction. This concept is illustrated in Figure 5a. Previous studies have suggested that such a chain can form at each end of the contacts^{32–34} and can reach several atoms in length at room temperature.³² Given that the atomic distance between gold atoms is approximately 0.236 nm, a gold chain of only a single atom at either end of the junction could easily

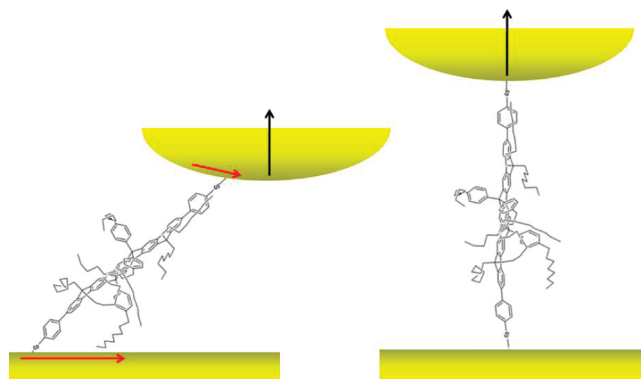


Figure 6. Schematic illustration of proposed molecular junction evolution. As the tip retracts, the molecule slides along the surface of the substrate so that it is pulled upright.

explain the observed steps that exceed the theoretical length of the 1-mer wire.

The histograms shown in Figure 5c all show a median step length significantly less than the theoretical length of the molecule. We propose a “sliding model”, illustrated in Figure 6, to explain the evolution of the molecular junction. The sliding model we describe here is similar to those proposed previously.^{35,36} In this model, the molecules are inhibited from standing upright on the surface due to their length; however, their alkyl side chains also prevent them from lying flat on the surface of the substrate. As a result, the molecules form a monolayer at an angle to the substrate when the molecular junction first forms. The retraction of the tip serves to pull the molecule in the junction into an upright position by sliding the gold–sulfur bond on the surface so that it is positioned under the apex of the tip. The fluctuations shown in the decay curves in Figure 5a,b can be partially attributed to the gold–sulfur bond sliding along the surface of the substrate as the tip retracts. Sliding is more difficult for longer molecules which inherently contain more degrees of freedom and are more likely to couple to the substrate. These factors may explain why the median step length in Figure 5c decreases for longer molecules. While local heating in molecular junctions is known to affect junction stability,³⁷ it is unlikely to have affected the junction stability of the longer molecules because heating is the result of current through the molecule and applied bias, and in our system of molecular wires the current decreases substantially with the molecular length even as the bias is increased.

Conclusion

The STM break junction technique was used to study the electrical properties of a family of molecular wires from 3.1 to 9.4 nm in length. The results showed highly length dependent and temperature invariant behavior in the shortest two wires and weakly length dependent and temperature variant behavior in the longer two wires. These data are consistent with a model whereby conduction is dominated by a coherent tunneling process in the shortest two wires and transitions to an incoherent hopping process in the longer two wires. To the best of our

- (32) Paulsson, M.; Krag, C.; Frederiksen, T.; Brandbyge, M. *Nano Lett.* **2009**, 9 (1), 117–121.
 (33) Xu, B. Q.; Xiao, X. Y.; Tao, N. J. *J. Am. Chem. Soc.* **2003**, 125 (52), 16164–16165.
 (34) Yamada, R.; Kumazawa, H.; Noutoshi, T.; Tanaka, S.; Tada, H. *Nano Lett.* **2008**, 8 (4), 1237–1240.

- (35) Kamenetska, M.; Koentopp, M.; Whalley, A. C.; Park, Y. S.; Steigerwald, M. L.; Nuckolls, C.; Hybertsen, M. S.; Venkataraman, L. *Phys. Rev. Lett.* **2009**, 102 (12), 126803.
 (36) Haiss, W.; Nichols, R. J.; van Zalinge, H.; Higgins, S. J.; Bethell, D.; Schiffrin, D. J. *Phys. Chem. Chem. Phys.* **2004**, 6 (17), 4330–4337.
 (37) Huang, Z. F.; Xu, B. Q.; Chen, Y. C.; Di Ventra, M.; Tao, N. J. *Nano Lett.* **2006**, 6 (6), 1240–1244.

knowledge, the last wire in the series represents the longest molecule measured by formation of a single-molecule junction. We found that the transition in charge transport behavior occurs between wires measuring 5.2 and 7.3 nm in length, which represents relatively long range tunneling. For the wires that conduct via hopping, the activation energy was measured to be between 0.52 and 0.58 eV. At elevated temperatures, charge hopping in the 3-mer wire can yield a higher conductance than nonresonant tunneling in the 2-mer wire. Analysis of the step length distribution showed that most steps were significantly shorter than the length of the molecule being measured. We feel that this phenomenon is best explained by sliding of the gold–sulfur bond across the substrate as the probe is retracted until either the bond stochastically breaks or the junction is mechanically broken.

Acknowledgment. We thank the U.S. National Science Foundation (Grant No. 0925498, T.H. and N.T.), U.S. Department of Energy (Grant No. DE-FG03-01ER45943, J.H. and N.T.), National Natural Science Foundation of China (Grant Nos. 20971025, 90922004, and 50903020, Z.-S.W. and G.Z.), and the International Outgoing Marie Curie Program within the 7th European Community framework for financial support.

Supporting Information Available: Information pertaining to analytical data for molecular wires 1–4, decay curve selection criteria, bias applied to the molecular junction, and electronic structure calculations for wires 1–3. This information is available free of charge via the Internet at <http://pubs.acs.org/>.

JA1040946